Similar turnover and shedding of the cellular prion protein in primary lymphoid and neuronal cells

Parizek, P; Roeckl, C; Weber, J; Flechsig, E; Aguzzi, A; Raeber, A J

Similar turnover and shedding of the cellular prion protein in primary lymphoid and neuronal cells

Abstract

The cellular prion protein (PrP(C)) is essential for pathogenesis and transmission of prion diseases. Although prion replication in the brain is accompanied by neurodegeneration, prions multiply efficiently in the lymphoreticular system without any detectable pathology. We have used pulse-chase metabolic radiolabeling experiments to investigate the turnover and processing of PrP(C) in primary cell cultures derived from lymphoid and nervous tissues. Similar kinetics of PrP(C) degradation were observed in these tissues. This indicates that the differences between these two organs with respect to their capacity to replicate prions is not due to differences in the turnover of PrP(C). Substantial amounts of a soluble form of PrP that lacks the glycolipid anchor appeared in the medium of splenocytes and cerebellar granule cells. Soluble PrP was detected in murine and human serum, suggesting that it might be of physiological relevance.

THE JOURNAL OF BIOLOGICAL CHEMISTRY
Vol. 276, No. 48, Issue of November 30, pp. 44627–44632, 2001

Printed in U.S.A.

Similar Turnover and Shedding of the Cellular Prion Protein in Primary Lymphoid and Neuronal Cells*

Received for publication, August 3, 2001, and in revised form, September 19, 2001
Published, JBC Papers in Press, September 24, 2001, DOI 10.1074/jbc.M107458200

Petra Parizek‡, Christiane Roeckl‡, Jacqueline Weber‡, Eckhard Flechsig§, Adriano Aguzzi‡, and Alex J. Raeber‡¶

From the ‡Institute of Neuropathology, Schmelzbergstr. 12, University Hospital, Zürich 8091, Switzerland and §Neurogenetics Unit, Imperial College of Medicine at St. Mary's, Norfolk Place, London W2 1PG, United Kingdom

The cellular prion protein (PrP^C) is essential for pathogenesis and transmission of prion diseases. Although prion replication in the brain is accompanied by neurodegeneration, prions multiply efficiently in the lymphoreticular system without any detectable pathology. We have used pulse-chase metabolic radiolabeling experiments to investigate the turnover and processing of PrP^C in primary cell cultures derived from lymphoid and nervous tissues. Similar kinetics of PrP^C degradation were observed in these tissues. This indicates that the differences between these two organs with respect to their capacity to replicate prions is not due to differences in the turnover of PrP^C. Substantial amounts of a soluble form of PrP that lacks the glycolipid anchor appeared in the medium of splenocytes and cerebellar granule cells. Soluble PrP was detected in murine and human serum, suggesting that it might be of physiological relevance.

Transmissible spongiform encephalopathies or prion disease are fatal neurological disorders that share the same basic pathogenic mechanisms, involving the structural conversion of the normal host prion protein (PrP^C)[1] into a protease-resistant form (PrP^{Sc}) (reviewed in Ref. 1). PrP^{Sc} is thought to be congruent with the infectious agent. The pathologic hallmarks of prion diseases are confined to the nervous system, where prions replicate efficiently. However in several mouse models of transmissible spongiform encephalopathies and in natural scrapie, as well as in variant Creutzfeldt-Jakob disease, prions replicate in lymphoid tissues long before infection spreads to the brain (2).

Some of the cell types involved in prion replication in nervous and lymphoid tissues have been elucidated. Using PrP knockout mice with ectopic, cell-restricted expression of PrP^C, it has been shown that in the brain, neurons (3) and astrocytes (4) are capable of propagating prions. In the lymphoreticular system, replication of some prion strains may be dependent on follicular dendritic cells (5), although this may not be a universal phenomenon (6, 7).

Little is known about the efficiency with which nervous and lymphoid cells replicate prions. It is conceivable that the early rise of infectivity titers in the lymphoreticular system (8) is due to a faster replication of prions in some cell types of the lymphoreticular system. It is also possible that increased turnover rates of PrP^C could result in an increased rate of conversion of PrP^C into PrP^{Sc}.

Studies with a neuroblastoma cell line showed that PrP^C is transported to the cell surface within 1 h of its synthesis and is degraded with a half-life of 3–6 h (9, 10). A small portion of PrP^C (10–30% of the cell surface pool) is shed into the medium by cultured cells (9–13). The released PrP^C may be produced by cleavage within the GPI region (13), or it may be shed into the medium after loss of its GPI anchor (12). Soluble forms of PrP^C have been identified not only in the medium of cultured cells but also in human cerebrospinal fluid (14) and have been released from human platelets (15).

Although these studies have shed some light on the cellular pathways of PrP biosynthesis and metabolism, they may not reflect completely the *in vivo* situation, and they do not address the importance of PrP expression and turnover in the lymphoreticular system (16–18), where prions replicate efficiently throughout the disease (8, 19).

In this report, we used primary splenocyte cultures to study the turnover of PrP^C in the lymphoreticular system and compared it with the turnover of PrP^C in primary cerebellar granule cell cultures. Both cell types showed similar turnover rates of PrP^C. We found that PrP^C turnover was significantly faster in primary cells than in cell lines of related origin. A substantial level of PrP was shed into the medium after loss of the GPI anchor. Shedding of PrP was found to be increased 3-fold in the presence of serum, suggesting that serum phospholipases might play a role in the shedding process.

MATERIALS AND METHODS

Primary Neuron Cultures—Cultures enriched in granule neurons were obtained from cerebella of 7-day-old mice as described previously (39). Briefly, cells were dissociated from freshly dissected cerebella by mechanical disruption in the presence of trypsin and DNase I. Cells were plated in Dulbecco's modified Eagle's medium (Life Technologies) supplemented with 10% fetal bovine serum, L-glutamine (Life Technologies), penicillin/streptomycin, and 25 mM KCl at a density of $3 \times 10^5/cm^2$ (2.5×10^6/35-mm dish).

CPs2 Cells—A PrP expression vector containing murine PrP driven by the CMV promoter was constructed by inserting the murine "half-genomic" PrP sequence as a blunted *Bam*HI-*Sal*I fragment excised from the plasmid pPrP-5′HG *Sal*I (19) into the *Sal*I-*Bgl*II restricted and blunted pAd-CMV-*lacZ* vector (40). The human retina cells 911 (41) were co-transfected with 3 μg of pAd-CMV-PrP HG *Sal* DNA and 0.6 μg of the plasmid pSV2neo carrying a neomycin resistance gene (42). Following calcium phosphate transfection, cells were split into three dishes and cultured in the presence of 0.9 mg/ml neomycin. After 3 weeks of selection, about 40–80 clones/plate were obtained in each

* This work was supported by the Kanton of Zürich and by grants of the Schweizerischer Nationalfonds (to A. J. R. and A. A.) and of the Migros and Coop foundations (to A. A.). The costs of publication of this article were defrayed in part by the payment of page charges. This article must therefore be hereby marked "*advertisement*" in accordance with 18 U.S.C. Section 1734 solely to indicate this fact.

¶ To whom correspondence should be addressed: Cytos Proteome Therapeutics GmbH, Fritz-Arnold-Str. 23, Konstanz 78467, Germany. Tel.: 49-7531-942-940; Fax: 49-7531-942-9422; E-mail: raeber@cytos.com.

[1] The abbreviations used are: PrP, prion protein; GPI, glycophosphatidylinositol; PAGE, polyacrylamide gel electrophoresis; CMV, cytomegalovirus.

transfection. Three bulk cultures for each construct were analyzed for PrP expression by flow cytometry. CPs2 cells were derived from a single cloned cell that was selected for high PrP expression using fluorescence-activated cell sorting with the polyclonal antibody 1B3 against mouse PrP (43) and a phycoerythrin-conjugated secondary antibody.

Metabolic Pulse-Chase Radiolabeling—Splenocyte cell suspensions were prepared from spleens of various mouse strains and used at 1–3 × 10^7 splenocytes/sample. Cerebellar granule cells were used at 10^6 cells/labeling experiment. Prior to labeling, cells were washed once with phosphate-buffered saline and starved for 30 min to 1 h at 37 °C in methionine/cysteine-free Dulbecco's modified Eagle's medium (Sigma) supplemented with 10% dialyzed fetal bovine serum (Sigma), 2 mM L-glutamine (Life Technologies), 2 mM L-cysteine (Life Technologies), and 10 mM Hepes buffer (pH 7.4) (Sigma). This medium was then replaced with 1 mCi of Tran[^{35}S]methionine (ICN Biomedicals)/ml in methionine-free Dulbecco's modified Eagle's medium containing the supplements described above for varied metabolic labeling times. At the end of the labeling period, cells were either washed once with cold phosphate-buffered saline, lysed, and processed for immunoprecipitation as described below or chased with cell culture medium (Dulbecco's modified Eagle's medium or RPMI) containing all of the supplements for the appropriate length of time. At different time points of the chase period, cells and medium were harvested and separated by centrifugation at 800 × *g* for 4 min.

Cell Lysis and Tissue Homogenates—Cells were lysed in lysis buffer (50 mM Tris-HCl, pH 7.5, 150 mM NaCl, 5 mM EDTA (TNE), 0.5% Nonidet P-40, 0.5% sodium deoxycholate, 0.1 mM phenylmethylsulfonyl fluoride, on ice for 5 min. The insoluble material was removed by centrifugation at 4000 × *g* for 10 min, and Sarkosyl was added to 0.4%.

Tissue homogenates (10%, w/v) of various mouse organs were prepared either in TNE (for brain) or phosphate-buffered saline (for spleen), both containing 2% Sarkosyl and 1 mM phenylmethylsulfonyl fluoride, by using an electric homogenizer (Polytron; Kinematica). The homogenates were cleared from insoluble material by centrifugation at 12,000–15,000 × *g* for 15 min.

Immunoprecipitation—To reduce nonspecific binding, radiolabeled proteins (500-μl aliquots of cell lysates or medium) were first preabsorbed with 20 μl of Gamma-Bind-Plus Sepharose (Amersham Pharmacia Biotech) for 1 h at 4 °C. Sepharose beads were centrifuged at 13,000 × *g* for 1 min, and the supernatant was used for immunoprecipitation.

For detection of PrP, polyclonal anti-PrP antibody R340 (20 μg) was added to the medium or lysate, and, after overnight incubation at 4 °C, the protein-antibody complexes were absorbed to Gamma-Bind-Plus Sepharose (40 μl/500 μl of solubilized protein) for 2 h at 4 °C. After centrifugation at 13,000 × *g* for 1 min, Sepharose-absorbed proteins were washed twice with lysis buffer containing 0.4% Sarcosyl, followed by two wash steps in high salt buffer (50 mM Tris-HCl, pH 7.5, 500 mM NaCl, 0.1% Nonidet P-40, 0.05% sodium deoxycholate) and one wash step in low salt buffer (50 mM Tris-HCl, pH 7.5, 0.1% Nonidet P-40, 0.05% sodium deoxycholate). All wash steps were performed at room temperature for 10 min each using a roller shaker. The Sepharose was resuspended in 3× loading buffer (1× loading buffer: 50 mM Tris-HCl, pH 6.8, 2% SDS, 0.1% bromphenol blue, 10% glycerol), boiled for 4–5 min, and analyzed by 12% SDS-PAGE (44).

For the immunoprecipitation of PrP from mouse and human plasma, the monoclonal antibody 6H4 (45) was first coupled to cyanogen bromide-activated Sepharose 4B (Amersham Pharmacia Biotech). The coupling procedure for 6H4 to cyanogen bromide-activated Sepharose and the preparation of Tris-inactivated Sepharose, used as a negative control and for preabsorption, were performed as described in the manual except that only 2 mg of 6H4 antibody/ml of gel were used for coupling. The immunoprecipitation was carried out as described above for the R340 antibody except for the following modifications. Preabsorption was performed with 40 μl of Tris-inactivated cyanogen bromide-activated Sepharose, and for the detection of PrP, 80 μl (~20 ng) of 6H4-Sepharose were used.

Detection of Proteins by Autoradiography—After SDS-PAGE, proteins were fixed, and the gel was incubated with fluorographic reagent (Amplify from Amersham Pharmacia Biotech) and dried according to the manual provided by the company. The gel was exposed to an x-ray film, or the autoradiographic signals were quantitated by densitometric analysis using phosphorimaging (Fujix Bas 2000). The amount of cellular and soluble PrP present at a time point during chase incubations is expressed as a percentage of the quantity of the nascent PrP recovered at the end of the pulse-labeling period.

Separation of Blood—Heparinized mouse blood (~1 ml) was taken by heart puncture and centrifuged twice at 2,000 × *g* for 10 min followed by 14,000 × *g* for 10 min. Supernatant (serum) was collected after each centrifugation step and finally analyzed by immunoprecipitation and Western blotting.

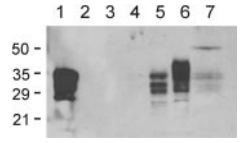

FIG. 1. **Expression levels of PrP^C in tissues of wild-type and transgenic mice.** Aliquots (25 μg of total protein) of brain or spleen homogenates were loaded in each lane. PrP was detected on blots with 1:5000 diluted polyclonal anti-PrP antiserum 1B3 (43). *Lane 1*, wild-type ($Prnp^{+/+}$) brain; *lane 2*, $Prnp^{0/0}$ brain; *lane 3*, $Prnp^{0/0}$ spleen; *lane 4*, $Prnp^{+/+}$ spleen; *lane 5*, *tga20* spleen; *lane 6*, Tg94/IRF spleen; *lane 7*, $Prnp^{+/+}$ spleen (175 μg of total protein). The positions of molecular mass markers in kDa are designated on the *left*.

Heparinized human peripheral blood (6 ml) was collected and separated with Lympholyte-H (Cedarlane Laboratories) density gradient centrifugation. The separation was performed according to the instructions provided by the manufacturer.

Analysis of PrP^C Hydrophobicity Using Triton X-114 Phase Partitioning—A working stock solution of Triton X-114 was prepared as described by Borchelt *et al.* (12); a 3% aqueous solution of Triton X-114 was mixed at 4 °C to solubilize the detergent. During an overnight incubation at 37 °C, the solution separated into a large aqueous phase and a smaller detergent phase. The aqueous phase was discarded, and the detergent phase was mixed with 0.1 volume of 10× TNE to give the Triton X-114 working stock.

To examine the hydrophobic properties of cellular proteins, cells were lysed in TNE containing 0.25 volumes of Triton X-114 stock. The proteins in medium were analyzed by first adding 0.1 volume of 10× TNE and then 0.25 volume of Triton X-114 stock. All samples were cooled to 4 °C and centrifuged at 3000 × *g* for 10 min at 4 °C to remove any insoluble aggregates. The supernatant was heated to 37 °C to induce phase transition and then centrifuged at 3000 × *g* for 10 min. The upper aqueous phase was transferred into a new tube, again mixed with 0.25 volume of Triton X-114 at 4 °C, and then heated to induce phase transition. The partitioning of the aqueous phase was repeated two more times to produce four separate detergent phases and one single aqueous phase. Proteins of each phase were precipitated with 5 volumes of methanol before immunopurification.

RESULTS

In wild-type mice, the highest concentration of PrP^C was found in the nervous system (Fig. 1, *lane 1*), whereas expression in wild-type spleen was barely detectable by immunoblot analysis (Fig. 1, *lanes 4* and *7*). Tga20 transgenic mice express at least 10 times more PrP^C in the spleen than wild-type mice (Fig. 1, *lane 5*) due to a high copy number of a PrP transgene (20). Expression of PrP^C in Tg94/IRF mice is driven by the interferon regulatory factor-1 promoter and the Eμ enhancer, which results in 1000-fold higher levels of PrP^C in the spleen (Fig. 1, *lane 6*) compared with wild-type mice (19). Surprisingly, the PrP glycosylation pattern of Tg94/IRF splenocytes differs from the pattern found in *tga20* transgenic mice. Most likely, this reflects cell-specific glycosylation, indicating that different cell populations express PrP in these transgenic mice (19).

Turnover of PrP^C in Primary Splenocyte Cultures of Tg94/IRF Mice—We used metabolic pulse-chase radiolabeling experiments to examine the biosynthesis and degradation of PrP^C in the lymphoreticular system. Initial attempts to metabolically radiolabel PrP in splenocytes prepared from wild-type mice failed due to the low expression level of PrP in wild-type spleen (data not shown). We then used primary cultures derived from spleens of Tg94/IRF mice, which overexpress about 1000-fold more PrP in the spleen than wild-type mice (19). PrP was pulse-labeled with [^{35}S]methionine for 3 h followed by a chase period of up to 17 h in complete medium supplemented with an excess of unlabeled methionine. The radiolabeled PrP was then immunoprecipitated with polyclonal antibody R340 (21) and analyzed by SDS-PAGE and fluorography. The autoradiograph

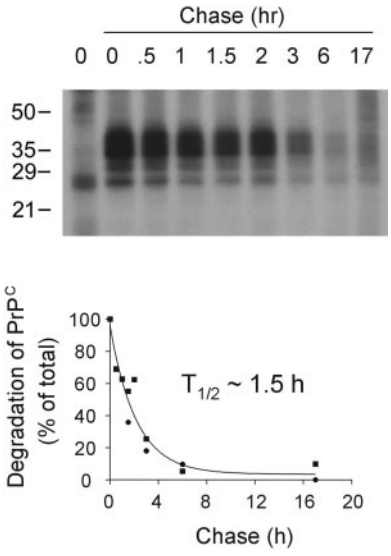

FIG. 2. **Degradation of PrP^C in splenocytes derived from Tg94/IRF transgenic mice.** 2×10^7 splenocytes were metabolically radiolabeled for 3 h with [^{35}S]methionine and then chased in complete medium for increasing periods of time. Cells were harvested at the indicated chase time, and cell lysates were used for immunoprecipitation with the anti-PrP serum R340. PrP was visualized by SDS-PAGE and fluorography. The *first lane* to the *left* is a negative control of *Prnp$^{0/0}$* splenocytes lysed and immunoprecipitated at the end of the pulse. The position of molecular mass markers are designated in kDa on the *left*. Data from two experiments were quantitated by phosphorimager analysis, and the values were plotted as a function of the chase period. The values for PrP^C are expressed as a percentage of the signal detected at the end of the pulse labeling period. The data points were fitted to an exponential curve using nonlinear regression analysis.

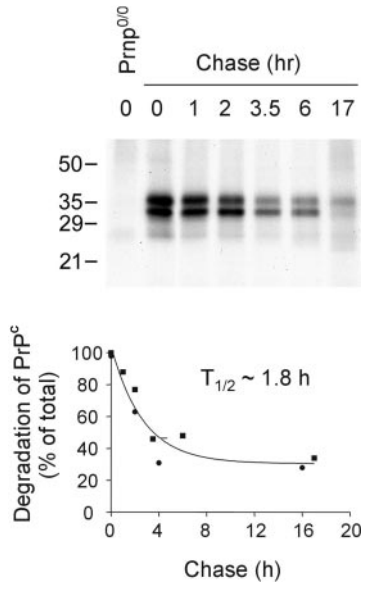

FIG. 3. **Degradation of PrP^C in splenocytes derived from *tga20* transgenic mice.** 2×10^7 splenocytes were metabolically radiolabeled for 3 h with [^{35}S]methionine and then chased in complete medium for increasing periods of time. Cells were harvested at the indicated chase time, and cell lysates were used for immunoprecipitation with the anti-PrP serum R340. PrP was visualized by SDS-PAGE and fluorography. The *first lane* to the *left* is a negative control of *Prnp$^{0/0}$* splenocytes lysed and immunoprecipitated at the end of the pulse. The position of molecular mass markers are designated in kDa on the *left*. Data from two experiments were quantitated and analyzed as described in Fig. 2.

shown in Fig. 2 as well as that from a similar experiment was analyzed by phosphorimaging, and the signals for the various glycosylated PrP isoforms were plotted as the fraction of the signal observed at the end of the pulse period. The two sets of data points show a great degree of reproducibility and can be fit by a line for exponential decay using nonlinear regression analysis. This analysis revealed a half-life for the newly synthesized PrP in Tg94/IRF splenocytes of 1.5 h (Fig. 2). These results indicate a faster degradation of cellular PrP in Tg94/IRF splenocytes compared with the N2a neuronal cell line in which PrP is degraded with a half-time of 3–6 h (9, 10).

Turnover of PrP^C in Primary Splenocyte Cultures of tga20 Mice—Since PrP expression in Tg94/IRF splenocytes is driven by a heterologous promoter, which results in at least 1000-fold higher levels of PrP^C in the spleen compared with wild-type mice, we asked whether the biosynthesis and degradation of PrP^C had been influenced by the IRF-1 promoter or by the strong overexpression of PrP^C. Therefore, we performed similar experiments with splenocytes from *tga20* transgenic mice. *tga20* mice harbor multiple copies of a PrP transgene containing the native promoter and express ~10-fold more PrP^C in the spleen than wild-type mice (Fig. 1). Following a 3-h pulse with [^{35}S]methionine, PrP^C in *tga20* splenocytes disappeared with a half-time of 1.8 h (Fig. 3). These results confirm that turnover of PrP in splenocytes is significantly faster than what was reported for neuronal tumor cell lines. To exclude the possibility that overexpression of PrP results in an increased turnover of PrP, we studied PrP degradation in CPs2 cells, a human retina cell line, which overexpress murine PrP at a similar level as Tg94/IRF splenocytes. However, radiolabeling studies in CPs2 cells showed that PrP was degraded with a half-time of 5–6 h (data not shown), which is similar to the findings of PrP degradation in neuroblastoma cells.

PrP^C Turnover in Cerebellar Granule Cells—We next asked whether the fast turnover of cell-associated PrP is specific for lymphoid cells. If this were the case, it might explain why prions multiply more efficiently in lymphoid tissues than in nervous tissues. To that purpose, we investigated the metabolism of PrP^C in nontumorigenic cells of the nervous system. We prepared primary cultures of cerebellar granule cells (CGC) from *tga20* transgenic mice. CGC were radiolabeled with [^{35}S]methionine for 3 h and chased up to 19 h (Fig. 4). Immunoprecipitation of radiolabeled PrP^C and quantitation by phosphorimaging revealed a half-life of 1.8 h for cell-associated PrP, which is similar to the kinetics for PrP disappearance in splenocytes. Therefore, we conclude that PrP^C is metabolized with similar kinetics in both lymphoid and nervous tissue but is more efficiently turned over in primary cells than in immortalized cell lines.

Release of PrP^C from Primary Lymphoid and Neuronal Cells—The mature form of PrP is attached to the cell surface by a glycolipid. In neuronal cell lines as well as in hamster brain, it has been shown that a form of PrP that lacks the GPI anchor is shed into the extracellular space (10, 12, 13). Furthermore, a soluble, N-terminally truncated form of PrP is released from human platelets. Interestingly, this processed soluble form of PrP that starts at Gly^{90} showed an electrophoretic mobility on SDS-PAGE similar to PrP$^{27–30}$, the protease-resistant core of PrP^{Sc} (15). Using a time-resolved fluoroimmunoassay, MacGregor *et al.* (22) showed that soluble forms of PrP are present in various human blood fractions. It is still unclear whether soluble PrP can be converted into PrP^{Sc}.

We examined the kinetics of the appearance of soluble forms of PrP released from metabolically radiolabeled Tg94/IRF splenocytes. Radiolabeled PrP was recovered from the medium after various chase time points by immunoprecipitation. Labeled PrP^C was first detected at 1 h of chase period, and maximal levels were present in the medium at 6 h. About 75% of the total labeled PrP^C was found to be accumulated in the medium at the end of the chase time (Fig. 5). The same analysis

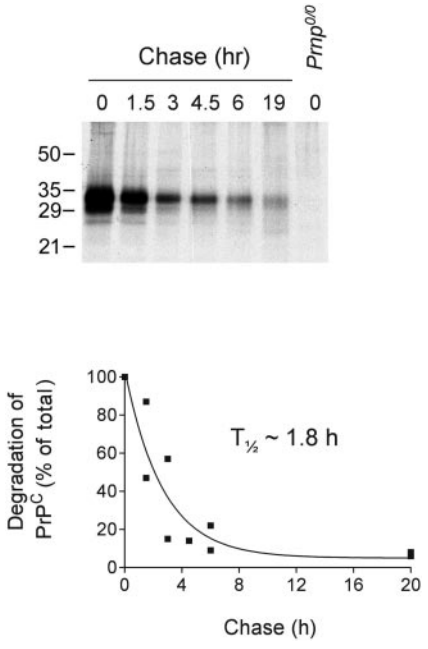

FIG. 4. **Degradation of PrP^C in cerebellar granule cells derived from *tga20* transgenic mice.** 10^6 cerebellar granule neurons were metabolically radiolabeled for 3 h with [^{35}S]methionine and then chased in complete medium for increasing periods of time. Cells were harvested and lysed at the indicated chase time, and 1 ml (of 1.5 ml) of cell lysate was used for immunoprecipitation with the anti-PrP serum R340. PrP was visualized by SDS-PAGE and fluorography. The positions of molecular mass markers are designated in kDa on the *left*. Data from one experiment were quantitated and analyzed as described in the legend to Fig. 2.

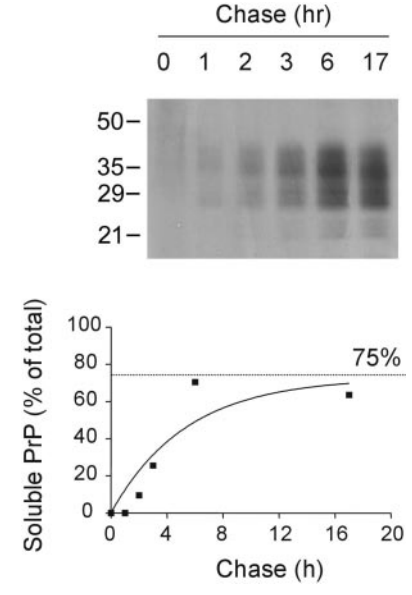

FIG. 5. **Release of PrP^C from splenocytes derived from Tg94/IRF transgenic mice.** 2×10^7 splenocytes were metabolically radiolabeled for 3 h with [^{35}S]methionine and then chased in complete medium for increasing periods of time. One-third of the medium was harvested at the indicated chase time and PrP immunoprecipitated with the anti-PrP serum R340. PrP was visualized by SDS-PAGE and fluorography. The position of molecular mass markers are designated in kDa on the *left*. Data from two experiments were quantitated and analyzed as described in the legend to Fig. 2.

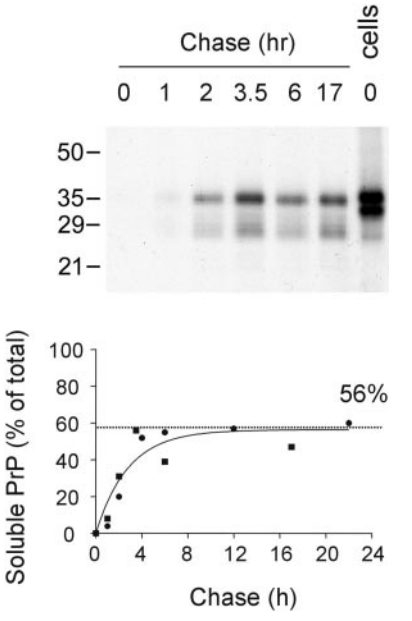

FIG. 6. **Release of PrP^C from splenocytes derived from *tga20* transgenic mice.** 2×10^7 splenocytes were metabolically radiolabeled for 3 h with [^{35}S]methionine and then chased in complete medium for increasing periods of time. One-third of the medium was harvested at the indicated chase time, and PrP was immunoprecipitated with the anti-PrP serum R340. PrP was visualized by SDS-PAGE and fluorography. The positions of molecular mass markers are designated in kDa on the *left*. Data from two experiments were quantitated and analyzed as described in Fig. 2.

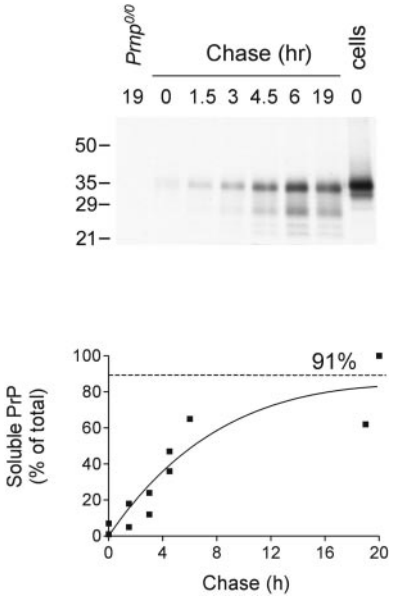

FIG. 7. **Release of PrP^C from cerebellar granule neurons derived from *tga20* transgenic mice.** 10^6 cerebellar granule neurons were metabolically radiolabeled for 3 h with [^{35}S]methionine and then chased in complete medium for increasing periods of time. Medium was collected at the indicated chase time, and 1 ml (of 1.5 ml) of medium was used for immunoprecipitation with the anti-PrP serum R340. PrP was visualized by SDS-PAGE and fluorography. The positions of molecular mass markers are designated in kDa on the *left*. Data from two experiments were quantitated and analyzed as described in the legend to Fig. 2.

was performed with splenocytes (Fig. 6) and CGC (Fig. 7) of *tga20* mice. Immunoprecipitation of labeled PrP^C from the medium showed that PrP^C is shed into the medium reaching a maximal level of 56 and 91%, respectively, of the total labeled cell-associated PrP^C present at the end of the pulse period. Interestingly, PrP^C shed from *tga20* splenocytes migrated predominantly as a single band around 35 kDa, corresponding to the diglycosylated form, and the low molecular weight species of PrP^C found associated with the cells was almost completely absent in the medium. The low molecular weight form may

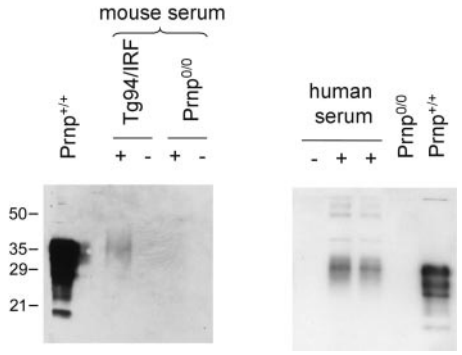

FIG. 8. **Detection of soluble PrP in serum of humans and transgenic Tg94/IRF mice.** Serum was separated from peripheral blood cells by centrifugation, and PrP was immunoprecipitated with the monoclonal anti-PrP antibody 6H4 covalently linked to Sepharose (+). As a negative control, some samples were treated with unconjugated Sepharose (−). Aliquots (20 μg of total protein) of wild-type ($Prnp^{+/+}$) or PrP knockout ($Prnp^{0/0}$) mouse brain homogenates were directly loaded onto the gel as controls. Following SDS-PAGE, PrP was visualized by Western blot analysis using the polyclonal anti-PrP serum 1B3. The positions of molecular mass markers are indicated in kDa on the *left*.

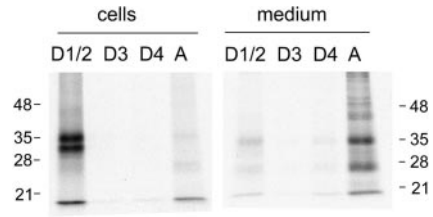

FIG. 9. **Shed PrP from splenocytes lacks the glycolipid anchor.** *tga20* splenocytes were metabolically radiolabeled for 3 h with [^{35}S]methionine (*cells*) followed by a chase period of 4–24 h (*medium*). Cells (2×10^7) and medium (from 4×10^7 cells) were extracted in Triton X-114 and partitioned to examine the Triton X-114 partitioning properties of cell-associated and soluble PrP. Protein from the aqueous (*A*) and the three subsequent Triton X-114 detergent phases (D1/2, D3, and D4) were concentrated by methanol precipitation before immunopurification with the polyclonal anti-PrP serum R340, and PrP was visualized by SDS-PAGE and fluorography. The positions of molecular mass markers are designated in kDa.

represent incompletely processed PrP molecules that are retained in the cell and cannot be released.

Soluble PrP in Blood of Mice and Humans—Detection of soluble PrP^C in the culture medium of splenocytes suggested that shedding of PrP^C is part of a processing pathway in the lymphoid system leading to the accumulation of significant levels of soluble PrP in the blood (22). To verify the presence of soluble PrP^C in serum, we examined mouse and human blood. Serum of Tg94/IRF mice was obtained by centrifugation of whole blood to remove white blood cells and erythrocytes. PrP^C was immunoprecipitated from the serum with the monoclonal antibody 6H4. Western blot analysis of the immunoprecipitates revealed a faint PrP band in the Tg94/IRF plasma, whereas control immunoprecipitates from $Prnp^{0/0}$ serum showed no corresponding signal (Fig. 8). Similarly, PrP was immunoprecipitated from human serum using 6H4-Sepharose and showed on immunoblots an array of bands around 35 kDa (Fig. 8). Control immunoprecipitations with Sepharose alone did not show any bands on the Western blot. PNGase F treatment of serum PrP resulted in a single band of 28 kDa representing the unglycosylated form of PrP, demonstrating that the heterogeneity of the PrP bands is due to various degrees of *N*-linked glycosylation (data not shown) (23–25). The fact that substantial amounts of soluble PrP were found in plasma of mice and humans suggests that shed PrP might be of physiological relevance.

It has been shown that shed PrP from primary cultures of neonatal hamster brain lacks the GPI anchor (12). Whether PrP shedding in the lymphoreticular system involves a similar processing event is still elusive. To determine whether release of PrP from lymphoid cells involves removal of the glycolipid moiety, we carried out Triton X-114 phase partitioning (26) of radiolabeled PrP^C from splenocytes and conditioned medium. We found that the majority of the cell-associated PrP partitioned into the detergent phase (D1/2; Fig. 9), characteristic of the GPI-modified protein. In contrast, most of the soluble PrP in the medium partitioned in the aqueous phase (*A*, Fig. 9), indicating that these PrP molecules lack the GPI anchor. We conclude that most of the PrP molecules released from splenocytes have lost their GPI moiety, suggesting that membrane-anchored PrP is processed to yield nonanchored, hydrophilic forms of PrP that are released into the medium.

DISCUSSION

In the present study, we have investigated the metabolism of PrP^C in primary cells derived from lymphoid tissue and compared it with the turnover of PrP^C in nervous tissue. Since PrP^C is the precursor in the conversion of PrP^C into the pathologic isoform PrP^{Sc}, the kinetics of PrP^C metabolism could hold important clues with regard to the efficiency of PrP^{Sc} and prion synthesis in different tissues.

PrP^C metabolism was studied in primary splenic cultures of two different transgenic mice, *tga20* and Tg94/IRF, which overexpress PrP^C in the spleen about 10- and 1000-fold, respectively, compared with wild-type mice (19, 20). In both transgenic mice, the half-life for the disappearance of PrP in splenocytes was found to be 1.5–2 h. The finding that PrP^C turnover is faster in splenocytes than in immortalized neuronal cells suggested that the processing and possibly also the conversion of PrP^C into PrP^{Sc} could be faster in lymphoid tissues. We therefore examined the kinetics of PrP^C metabolism in primary cerebellar granule cell cultures. Our results showed that, similarly to splenocytes, primary neuronal cells showed a half-time for PrP^C degradation of 1.5–2 h. Since PrP^C turnover in splenocytes is similar to the turnover in granule cells, turnover of PrP^C seemed not to be responsible for the fast replication of prions in the lymphoid system. However, it is also possible that turnover of PrP in splenocyte cultures mainly reflects turnover of PrP in lymphocytes, which may not be relevant for prion replication, but these constitute more than 90% of the cells in splenocyte cultures (27). It has been shown that neither T (19) nor B cells (28) are capable of prion replication. On the other hand, FDCs that have been incriminated to play a crucial role in prion replication (5, 29–31) constitute less than 1% of the cells in secondary lymphoid organs and are known to be difficult to isolate in an intact form (27).

The fast degradation of PrP in primary tissues is in contrast to studies of PrP metabolism in cultured neuroblastoma cells, where PrP is degraded with a half-time of 3–6 h (9, 10). It is possible that the overexpression of PrP could be responsible for this discrepancy. However, we found that PrP in human retina CPs2 cells that overexpress mouse PrP at a similar level as Tg94/IRF splenocytes was degraded with a half-time of 5–6 h as reported for mouse neuroblastoma cells. These results suggest that overexpression of PrP is not responsible for the fast degradation rate of PrP in primary tissues. Furthermore, these findings support the notion that PrP^C is degraded faster in primary cells than in the cell lines that were reported before (9, 10).

Earlier studies showed that several GPI-anchored glycoproteins are shed from the cell membrane and exist as soluble

proteins *in vitro* and *in vivo* (32, 33). In addition, there is evidence for a soluble form of PrP^C in the medium of cultured cells (9–13), in human cerebrospinal fluid (14), in human blood (22), and released from activated human platelets (15).

To investigate whether shedding of PrP is a physiologically relevant processing pathway for PrP, we metabolically labeled splenocytes of Tg94/IRF and *tga20* transgenic mice and followed the release of a soluble form of PrP^C into the medium. A soluble form appeared as early as 2 h after starting the chase period and was present at a level corresponding to 60–70% of the labeled cellular PrP^C, which is in stark contrast to earlier findings in neuroblastoma cells, where only 10–30% of the cellular PrP^C was shed into the medium (9–13). Since in some of these studies serum was omitted from the chase medium, the high levels of shed PrP were possibly due to the presence of serum in the chase medium. We carried out radiolabeling experiments in CPs2 cells and performed chase incubations with or without serum. Without serum, about 5% of the total labeled PrP was shed after 17 h of chase, whereas about 15% of the total labeled PrP was released into the medium with serum (data not shown). These results suggest that serum enzymes such as phosphatidylinositol-specific phospholipase C or D might be involved in the release of PrP from cells. A number of GPI-anchored proteins on lymphocytes have been shown to be released by phospholipases in the serum and to exert important signaling functions in the lymphoid system (34). Whether soluble PrP has such a function remains to be seen.

Our finding that substantial amounts of shed PrP are present in serum of mice and humans raises the question of whether soluble PrP can be converted into PrP^{Sc}. Although firm evidence for the presence of prion infectivity in blood is still missing, it was recently shown that blood from bovine spongiform encephalopathy-infected cattle can transmit the disease to sheep (35). This scenario has far reaching consequences for public health, because it would suggest that blood donors subclinically infected with the bovine spongiform encephalopathy agent could potentially transmit variant Creutzfeldt-Jakob disease via blood transfusion to healthy individuals. This stresses the urgent need to develop sensitive tests for the detection of prions in body fluids. Several recent reports raise hope that this should be accomplished in the not too distant future. An erythroid-specific transcript, erythroid differentiation-related factor, was shown to be down-regulated in the blood of scrapie-infected sheep (36). This might represent a valuable diagnostic marker to screen the blood supply. Improved diagnostic tests could now be developed using a new cyclic amplification procedure, which is capable of efficiently amplifying minute amounts of PrP^{Sc} in brain tissue (37). Coupled with a reagent that specifically binds to PrP^{Sc}, such as the recently identified plasminogen (38), this might reveal the levels of prion infectivity looming in the blood.

Acknowledgments—We thank C. Weissmann for critical comments and C. Farqhuar for the 1B3 antibody.

REFERENCES

1. Aguzzi, A., Montrasio, F., and Kaeser, P. S. (2001) *Nat. Rev. Mol. Cell. Biol.* **2,** 118–126
2. Raeber, A. J., and Aguzzi, A. (2000) *Immunol. Today* **21,** 66–67
3. Race, R. E., Priola, S. A., Bessen, R. A., Ernst, D., Dockter, J., Rall, G. F., Mucke, L., Chesebro, B., and Oldstone, M. B. (1995) *Neuron* **15,** 1183–1191
4. Raeber, A. J., Race, R. E., Brandner, S., Priola, S. A., Sailer, A., Bessen, R. A., Mucke, L., Manson, J., Aguzzi, A., Oldstone, M. B., Weissmann, C., and Chesebro, B. (1997) *EMBO J.* **16,** 6057–6065
5. Brown, K. L., Stewart, K., Ritchie, D. L., Mabbott, N. A., Williams, A., Fraser, H., Morrison, W. I., and Bruce, M. E. (1999) *Nat. Med.* **5,** 1308–1312
6. Blättler, T., Brandner, S., Raeber, A. J., Klein, M. A., Voigtländer, T., Weissmann, C., and Aguzzi, A. (1997) *Nature* **389,** 69–73
7. Kaeser, P. S., Klein, M. A., Schwarz, P., and Aguzzi, A. (2001) *J. Virol.* **75,** 7097–7106
8. Eklund, C. M., Kennedy, R. C., and Hadlow, W. J. (1967) *J. Infect. Dis.* **117,** 15–22
9. Borchelt, D. R., Scott, M., Taraboulos, A., Stahl, N., and Prusiner, S. B. (1990) *J. Cell Biol.* **110,** 743–752
10. Caughey, B., Race, R. E., Ernst, D., Buchmeier, M. J., and Chesebro, B. (1989) *J. Virol.* **63,** 175–181
11. Caughey, B. (1993) *Br. Med. Bull.* **49,** 860–872
12. Borchelt, D. R., Rogers, M., Stahl, N., Telling, G., and Prusiner, S. B. (1993) *Glycobiology* **3,** 319–329
13. Harris, D. A., Huber, M. T., van Dijken, P., Shyng, S. L., Chait, B. T., and Wang, R. (1993) *Biochemistry* **32,** 1009–1016
14. Tagliavini, F., Prelli, F., Porro, M., Salmona, M., Bugiani, O., and Frangione, B. (1992) *Biochem. Biophys. Res. Commun.* **184,** 1398–1404
15. Perini, F., Vidal, R., Ghetti, B., Tagliavini, F., Frangione, B., and Prelli, F. (1996) *Biochem. Biophys. Res. Commun.* **223,** 572–577
16. Cashman, N. R., Loertscher, R., Nalbantoglu, J., Shaw, I., Kascsak, R. J., Bolton, D. C., and Bendheim, P. E. (1990) *Cell* **61,** 185–192
17. Holada, K., and Vostal, J. G. (2000) *Br. J. Haematol.* **110,** 472–480
18. Kubosaki, A., Yusa, S., Nasu, Y., Nishimura, T., Nakamura, Y., Saeki, K., Matsumoto, Y., Itohara, S., and Onodera, T. (2001) *Biochem. Biophys. Res. Commun.* **282,** 103–107
19. Raeber, A. J., Sailer, A., Hegyi, I., Klein, M. A., Rülicke, T., Fischer, M., Brandner, S., Aguzzi, A., and Weissmann, C. (1999) *Proc. Natl. Acad. Sci. U. S. A.* **96,** 3987–3992
20. Fischer, M., Rülicke, T., Raeber, A., Sailer, A., Moser, M., Oesch, B., Brandner, S., Aguzzi, A., and Weissmann, C. (1996) *EMBO J.* **15,** 1255–1264
21. Brandner, S., Isenmann, S., Raeber, A., Fischer, M., Sailer, A., Kobayashi, Y., Marino, S., Weissmann, C., and Aguzzi, A. (1996) *Nature* **379,** 339–343
22. MacGregor, I., Hope, J., Barnard, G., Kirby, L., Drummond, O., Pepper, D., Hornsey, V., Barclay, R., Bessos, H., Turner, M., and Prowse, C. (1999) *Vox. Sang.* **77,** 88–96
23. Endo, T., Groth, D., Prusiner, S. B., and Kobata, A. (1989) *Biochemistry* **28,** 8380–8388
24. Haraguchi, T., Fisher, S., Olofsson, S., Endo, T., Groth, D., Tarentino, A., Borchelt, D. R., Teplow, D., Hood, L., Burlingame, A., Haraguchi, T., Fisher, S., Olofsson, S., Endo, T., Groth, D., Tarentino, A., Borchelt, D. A., Teplow, D., Hood, L., Burlingame, A., Lycke, E., Kobata, A., and Prusiner, S. B. (1989) *Arch. Biochem. Biophys.* **274,** 1–13
25. Taraboulos, A., Rogers, M., Borchelt, D. R., McKinley, M. P., Scott, M., Serban, D., and Prusiner, S. B. (1990) *Proc. Natl. Acad. Sci. U. S. A.* **87,** 8262–8266
26. Bordier, C. (1981) *J. Biol. Chem.* **256,** 1604–1607
27. Schnizlein, C. T., Kosco, M. H., Szakal, A. K., and Tew, J. G. (1985) *J. Immunol.* **134,** 1360–1368
28. Montrasio, F., Cozzio, A., Flechsig, E., Rossi, D., Klein, M. A., Rulicke, T., Raeber, A. J., Vosshenrich, C. A., Proft, J., Aguzzi, A., and Weissmann, C. (2001) *Proc. Natl. Acad. Sci. U. S. A.* **98,** 4034–4037
29. Montrasio, F., Frigg, R., Glatzel, M., Klein, M. A., Mackay, F., Aguzzi, A., and Weissmann, C. (2000) *Science* **288,** 1257–1259
30. Klein, M. A., Kaeser, P. S., Schwarz, P., Weyd, H., Xenarios, I., Zinkernagel, R. M., Carroll, M. C., Verbeek, J. S., Botto, M., Walport, M. J., Molina, H., Kalinke, U., Acha-Orbea, H., and Aguzzi, A. (2001) *Nat. Med.* **7,** 488–492
31. Mabbott, N. A., Mackay, F., Minns, F., and Bruce, M. E. (2000) *Nat. Med.* **6,** 719–720
32. Mizukami, I. F., Faulkner, N. E., Gyetko, M. R., Sitrin, R. G., and Todd, R. F., III (1995) *Blood* **86,** 203–211
33. Smith, G. M., Biggs, J., Norris, B., Anderson-Stewart, P., and Ward, R. (1997) *J. Clin. Immunol.* **17,** 502–509
34. Lehto, M. T., and Sharom, F. J. (1998) *Biochem. J.* **332,** 101–109
35. Houston, F., Foster, J. D., Chong, A., Hunter, N., and Bostock, C. J. (2000) *Lancet* **356,** 999–1000
36. Miele, G., Manson, J., and Clinton, M. (2001) *Nat. Med.* **7,** 361–364
37. Saborio, G. P., Permanne, B., and Soto, C. (2001) *Nature* **411,** 810–813
38. Fischer, M. B., Roeckl, C., Parizek, P., Schwarz, H. P., and Aguzzi, A. (2000) *Nature* **408,** 479–483
39. Marini, A. M., and Paul, S. M. (1992) *Proc. Natl. Acad. Sci. U. S. A.* **89,** 6555–6559
40. Schneider, S. D., Rusconi, S., Seger, R. A., and Hossle, J. P. (1997) *Gene Ther.* **4,** 524–532
41. Fallaux, F. J., Kranenburg, O., Cramer, S. J., Houweling, A., Van Ormondt, H., Hoeben, R. C., and Van Der Eb, A. J. (1996) *Hum. Gene Ther.* **7,** 215–222
42. Southern, P. J., and Berg, P. (1982) *J. Mol. Appl. Genet.* **1,** 327–341
43. Farquhar, C. F., Somerville, R. A., and Ritchie, L. A. (1989) *J. Virol. Methods* **24,** 215–221
44. Laemmli, U. K. (1970) *Nature* **227,** 680–685
45. Korth, C., Stierli, B., Streit, P., Moser, M., Schaller, O., Fischer, R., Schulz-Schaeffer, W., Kretzschmar, H., Raeber, A., Braun, U., Ehrensperger, F., Hornemann, S., Glockshuber, R., Riek, R., Billeter, M., Wuthrich, K., and Oesch, B. (1997) *Nature* **390,** 74–77